

Strain-specific proteome responses of *Pseudomonas aeruginosa* to biofilm-associated growth and to calcium

Marianna A. Patrauchan,¹ Svetlana A. Sarkisova²
and Michael J. Franklin^{2,3}

Correspondence

Michael J. Franklin
umbfm@montana.edu

¹Department of Microbiology and Immunology, University of British Columbia, Vancouver, BC V6T 1Z3, Canada

²Department of Microbiology, Montana State University, Bozeman, MT 59717, USA

³Center for Biofilm Engineering, Montana State University, Bozeman, MT 59717, USA

Pseudomonas aeruginosa is an opportunistic pathogen that forms biofilms on mucous plugs in the lungs of cystic fibrosis (CF) patients, resulting in chronic infections. Pulmonary *P. aeruginosa* isolates often display a mucoid (alginate-producing) phenotype, whereas non-mucoid strains are generally associated with acute infections. We characterized the cytosolic proteomes of biofilm-associated and planktonic forms of a CF pulmonary isolate, *P. aeruginosa* FRD1, and a non-mucoid strain, PAO1. Since Ca²⁺ metabolism is altered in CF pulmonary fluids, we also analysed the effect of Ca²⁺ on the proteome responses of these strains. Both strains altered the abundances of 40–60 % of their proteins in response to biofilm growth and/or [Ca²⁺]. Differentially expressed proteins clustered into 12 groups, based on their abundance profiles. From these clusters, 146 proteins were identified by using MALDI-TOF/TOF mass spectrometry. Similarities as well as strain-specific differences were observed. Both strains altered the production of proteins involved in iron acquisition, pyocyanin biosynthesis, quinolone signalling and nitrogen metabolism, proteases, and proteins involved in oxidative and general stress responses. Individual proteins from these classes were highly represented in the biofilm proteomes of both strains. Strain-specific differences concerned the proteins within these functional groups, particularly for enzymes involved in iron acquisition and polysaccharide metabolism, and proteases. The results demonstrate that a mucoid CF isolate of *P. aeruginosa* responds to biofilm-associated growth and [Ca²⁺] in a fashion similar to strain PAO1, but that strain-specific differences may allow this CF isolate to successfully colonize the pulmonary environment.

Received 4 June 2007

Revised 23 July 2007

Accepted 26 July 2007

INTRODUCTION

Pseudomonas aeruginosa is an opportunistic pathogen that can cause a variety of biofilm-associated diseases, including infections in burn wounds and tissue injuries (Costerton *et al.*, 1995, 1999). *P. aeruginosa* is also one of the main organisms associated with pulmonary infections in patients undergoing immunosuppressive therapy, or patients with the genetic disorder cystic fibrosis (CF) (Lyczak *et al.*, 2000). The ability of *P. aeruginosa* to cause disease is due to multiple factors including its inherent resistance to many antibiotics and its ability to produce a large repertoire of secreted virulence factors, such as exotoxins, proteases, lipases and pyocyanin (Stover *et al.*, 2000). *P. aeruginosa*

also produces protective extracellular polysaccharides including alginate, Psl and Pel polysaccharides that contribute to biofilm formation (Friedman & Kolter, 2004; Hentzer *et al.*, 2001; Jackson *et al.*, 2004; Nivens *et al.*, 2001) and provide protection of the bacteria from host defensive responses (Lyczak *et al.*, 2002; Mai *et al.*, 1993; Pier *et al.*, 2001).

Biofilm-associated infections are particularly important, since the bacteria growing in biofilms are often highly resistant to antibiotics and to host innate defensive processes (Jesaitis *et al.*, 2003; Stewart & Costerton, 2001). It is not entirely clear why the bacteria in biofilms have these enhanced resistances. In the case of antibiotics, studies have demonstrated that most antibiotics are not diffusion limited, and therefore adequately penetrate biofilms (Rani *et al.*, 2005; Roberts & Stewart, 2004; Walters *et al.*, 2003). This suggests that bacterial physiology

Abbreviations: BMM, biofilm minimal medium; CF, cystic fibrosis; NV, normalized volume; PQS, *Pseudomonas* quinolone signal; 2DGE, two-dimensional gel electrophoresis.

may dictate antibiotic resistance in biofilms, mechanisms of which have been proposed. For example, biofilm-associated *P. aeruginosa* may produce cyclic glucans, not produced by planktonic cells, to increase resistance (Mah *et al.*, 2003). A subset of physiologically distinct bacteria with enhanced antibiotic resistance may repopulate biofilms following antibiotic treatment of the sensitive cells (Keren *et al.*, 2004; Lewis, 2007). Cells with differing physiological properties within biofilms have been described, even for originally clonal cultures (Boles *et al.*, 2004), suggesting that differences in antibiotic resistance may occur at the individual cell level. Although less well characterized, physiological properties of biofilm-associated bacteria may also influence the enhanced resistance of these bacteria to host defences (Jensen *et al.*, 2007; Jesaitis *et al.*, 2003). Since biofilm-associated *P. aeruginosa* appear to be physiologically different from cells in planktonic culture, several previous studies have used transcriptomic and proteomic approaches to identify changes in gene expression during *P. aeruginosa* biofilm development (Sauer *et al.*, 2002; Southey-Pillig *et al.*, 2005; Waite *et al.*, 2005, 2006; Whiteley *et al.*, 2001). Sauer *et al.* (2002) found that as much as 50% of the *P. aeruginosa* PAO1 proteome may differ during certain stages of biofilm development compared to planktonic cells. Some of these differences are likely to be responsible for the increased resistance of the bacteria to antibiotics and host defences.

Patients with CF are particularly susceptible to biofilm infections with *P. aeruginosa* due to mutations of the cystic fibrosis transmembrane regulator (CFTR), which lead to a build up of mucous in the pulmonary fluid (Lyczak *et al.*, 2000). Calcium metabolism disorder is central to the pathology of CF (von Ruecker *et al.*, 1984). Pulmonary fluid and nasal secretions in patients with CF contain elevated concentrations of Ca^{2+} (Halmerbauer *et al.*, 2000; Lorin *et al.*, 1976). Both Ca^{2+} influx and efflux increase in isolated CF mitochondria, resulting in net Ca^{2+} accumulation. Retention of CFTR in the endoplasmic reticulum is dependent upon chaperone proteins that require Ca^{2+} for optimal activity (Egan *et al.*, 2002). Ca^{2+} also influences migration of eosinophils across lung epithelium (Liu *et al.*, 1999). High levels of Ca^{2+} , Na^+ and Cl^- may influence release of cytotoxic eosinophil products, affecting mucociliary clearance and promoting epithelial-cell injury and fibrosis (Halmerbauer *et al.*, 2000).

We have recently described the extracellular constituents of two *P. aeruginosa* strains growing in biofilms and exposed to elevated $[\text{Ca}^{2+}]$ (Sarkisova *et al.*, 2005). Several findings were surprising. First, elevated $[\text{Ca}^{2+}]$ influenced biofilm architecture of both the alginate-producing CF isolate FRD1 and the non-mucoid strain PAO1. The effect was more dramatic for FRD1, with biofilms as much as 10-fold thicker when Ca^{2+} ions were added. This increased thickness was due primarily to increased biosynthesis of alginate, which was as much as eightfold induced in biofilms exposed to medium with Ca^{2+} . The PAO1 biofilm architecture was also influenced by Ca^{2+} , although to a

lesser extent, and without production of alginate. Second, calcium influenced the production of extracellular proteases (alkaline protease, elastase and PrpL protease), which accumulated in the biofilm alginate matrix of the mucoid strain FRD1. Previously, it was thought that there was an inverse relationship between alginate production and production of extracellular proteins. Although this is the case for certain environmental conditions, when Ca^{2+} is present, both alginate and proteases are highly upregulated in biofilms of the alginate-producing strain. Third, Ca^{2+} influenced the production of the secreted redox-active compound pyocyanin, which in turn may disrupt calcium homeostasis of epithelial cells (Denning *et al.*, 1998).

Calcium is an important signalling molecule in eukaryotic cells. It also plays a signalling role in bacteria, particularly in the case of secreted proteins (Marquart *et al.*, 2005; Olson & Ohman, 1992; Sarkisova *et al.*, 2005; Yahr *et al.*, 1997). Since Ca^{2+} influences biofilm architecture and production of extracellular matrix materials in *P. aeruginosa*, we chose to continue our studies on the physiological differences of biofilm-associated bacteria by investigating the effect of Ca^{2+} and biofilm growth of the *P. aeruginosa* cytosolic proteome. Here, we used high-resolution two-dimensional gel electrophoresis and algorithms for quantitative 2D gel digital image analysis as tools for discovery of cytosolic proteins influenced by calcium and biofilm-associated growth. We studied the responses of a mucoid CF pulmonary isolate, *P. aeruginosa* FRD1, and compared the results to those for a non-CF strain, PAO1. The goals were (i) to characterize the cytosolic proteome responses to two environmental factors important in CF pathogenesis (Ca^{2+} and biofilm growth), and (ii) to provide strain comparisons between two different and physiologically distinct *P. aeruginosa* isolates. This comparative analysis for a CF isolate is necessary for a deeper understanding of environmental stimuli and cell responses that drive successful acute and chronic *P. aeruginosa* biofilm infections.

METHODS

Bacterial strains and media. *Pseudomonas aeruginosa* FRD1 and PAO1 were used in this study. *P. aeruginosa* FRD1 is an alginate-overproducing (mucoid) CF pulmonary isolate (Ohman & Chakrabarty, 1981), and *P. aeruginosa* PAO1 is the non-mucoid strain used for the original genome sequencing study (Stover *et al.*, 2000). Biofilm minimal medium (BMM) contained (per litre): 9.0 mM sodium glutamate, 50 mM glycerol, 0.02 mM MgSO_4 , 0.15 mM NaH_2PO_4 , 0.34 mM K_2HPO_4 , 145 mM NaCl, 20 μl trace metal solution and 1 ml vitamin solution. Trace metal solution contained (per litre 0.83 M HCl): 5.0 g $\text{CuSO}_4 \cdot 5\text{H}_2\text{O}$, 5.0 g $\text{ZnSO}_4 \cdot 7\text{H}_2\text{O}$, 5.0 g $\text{FeSO}_4 \cdot 7\text{H}_2\text{O}$ and 2.0 g $\text{MnCl}_2 \cdot 4\text{H}_2\text{O}$. Vitamin solution contained (per litre): 0.5 g thiamine and 1 mg biotin. The pH of the medium was adjusted to 7.0. When required, $\text{CaCl}_2 \cdot 2\text{H}_2\text{O}$ was added to final concentration of 10.0 mM.

Biofilm growth. *P. aeruginosa* biofilms were cultivated on the walls of silicone tubing (0.6 m length, size 18 tubing with an interior volume of 40 ml), as in experiments described previously (Sarkisova

et al., 2005; Sauer *et al.*, 2002). Briefly, the system consisted of a single-flow-through system containing a medium reservoir, pump, silicone tubing and a waste container. Prior to inoculation into the system, each strain was incubated in BMM for 16–20 h at 37 °C. When the cell density reached 1×10^7 cells ml⁻¹, as determined by absorption/scattering, the cultures were diluted to 1×10^6 cells ml⁻¹ in 0.85 % NaCl. This culture (2 ml) was used to inoculate the tubing flow-cells under quiescent conditions for 20 min. Following inoculation, sterile BMM was pumped through the tubing at a rate of 2 ml min⁻¹ for 72 h to allow biofilm growth. Attached cells were removed from the interior surface of the tubing by using the plunger of a 3 ml syringe. Planktonic cultures were incubated in BMM medium at 37 °C as described previously (Sarkisova *et al.*, 2005). Cells were harvested from 500 ml flasks after 18 h growth (mid-exponential phase).

Two-dimensional gel electrophoresis (2DGE) of cellular proteins. Preliminary experiments indicated that most *P. aeruginosa* proteins resolved in the acidic-to-neutral range. Therefore, Pharmalyte and Immobiline Dry-Strips 4–7 (GE Healthcare) were used for isoelectric focusing. Iodacetamide and CHAPS were from Acros Organics and MP Biomedicals, respectively. All chemicals were of analytical grade and used without further purification.

Cells from planktonic and biofilm cultures were obtained as described previously (Sarkisova *et al.*, 2005). Cell pellets were washed twice with saline solution (0.85 % NaCl) and resuspended in TE buffer (10 mM Tris/HCl, 1 mM EDTA, pH 8.0, containing 0.3 mg PMSF ml⁻¹). Cells were disrupted by sonication (12 times for 10 s, 4 W, 4 °C), and the cell debris and unbroken cells were removed by centrifugation (12 000 g, 60 min, 4 °C). The protein concentrations of the supernatants were determined by using a modified Lowry assay. Protein samples were stored as aliquots at –80 °C. Two-dimensional gel electrophoresis was performed as described previously (Sarkisova *et al.*, 2005). Briefly, proteins were loaded by in-gel rehydration into 18 cm immobilized pH gradient (IPG) strips with pH range of 4–7. Solubilization buffer consisted of 9 M urea, 2 M thiourea, 4 % CHAPS, 2 % (w/v) carrier ampholytes, 0.037 M DTT and a trace amount of bromophenol blue. Isoelectric focusing was conducted using a Multiphor II (Pharmacia) at 20 °C. Proteins were focused for a total of 28 kVh. Second-dimension electrophoresis was carried out on 11 % polyacrylamide gels (230 × 200 × 1 mm) using a vertical Hoefer Dalt system (Pharmacia) at 10 °C using 10 mA per gel for 4 h, then 40 mA per gel for 14–16 h. Proteins were detected by colloidal Coomassie staining.

Proteomic analysis. The gels were imaged, and the digital images were analysed by using Progenesis Workstation software (Nonlinear Dynamics). A minimum of two biological replicates were performed for each condition, and the signal intensity of each spot was averaged over the replicates. The signal intensities of protein spots were normalized against total signal intensity detected on a gel. Only the proteins present in all replicates were added to the averaged gel, and only spots with a normalized volume (NV) of 0.01 or greater were analysed further. The averaged proteome profiles obtained for every condition were quantitatively compared. To analyse changes in protein abundance profiles across multiple proteomes, spots and normalized intensity values were imported into GeneSpring GXv7.3.1 software (Agilent Technologies). Normalized protein values were filtered for fold-change; those with at least a twofold change compared to any other sample were selected for cluster analysis. Primary clusters were obtained by hierarchical clustering of both genes and conditions, using a Pearson correlation similarity measure and an average linkage clustering algorithm. Clusters were manually refined on the basis of dominant fold-change differences between experimentally significant groups.

For protein identification we targeted proteins if they met two criteria: (1) the protein had a NV greater than 0.03, and (2) the proteins were at least threefold more or less abundant in the planktonic or biofilm proteomes cultivated with 10 mM CaCl₂ versus their matched counterparts cultivated without added CaCl₂. Proteins of interest were excised from the gels and identified based on peptide mass fingerprint analysed on a 4700 MALDI-TOF/TOF mass spectrometer (University of Texas, Biomolecular Resource facility, Mass Spectrometry Laboratory), using the Applied Biosystems GPS (version 3.6) software, MASCOT search engine and NCBI nr database. A protein was considered identified if the hit fulfilled four criteria: (1) it was statistically significant (with a MASCOT search score above 75), (2) the number of the matched peptides was at least five, (3) the protein sequence coverage was above 20 %, and (4) the predicted molecular mass and pI were consistent with the experimentally determined values.

RESULTS AND DISCUSSION

Biofilm growth and [Ca²⁺] have cumulative effects on the proteomes of *P. aeruginosa* PAO1 and FRD1

P. aeruginosa undergoes physiological changes during its transition from planktonic to biofilm-associated growth and chronic pulmonary infections. Proteomic and transcriptomic studies have been performed previously to study changes in non-mucoid strains during biofilm formation (Sauer *et al.*, 2002; Southey-Pillig *et al.*, 2005; Waite *et al.*, 2005, 2006; Whiteley *et al.*, 2001). In addition, transcriptional profiles have been obtained previously for mucoid *P. aeruginosa* (Firoved & Deretic, 2003). Here we present a global proteomic examination comparing an alginate-producing CF lung isolate and a non-mucoid strain of *P. aeruginosa* during growth in planktonic culture and in biofilms. The experiments were performed in minimal medium, so that the effects of additional environmental parameters could be determined. Our previous work identified Ca²⁺ as influencing biofilm structure of *P. aeruginosa*, and causing changes in the concentration of extracellular biofilm-matrix factors (Sarkisova *et al.*, 2005). Therefore, and for reasons described above, we chose to investigate the effect of Ca²⁺ on the global cytosolic factors of the two strains during biofilm growth.

Using 2DGE, we resolved on average 630 protein spots in the pH range 4–7 for the non-mucoid strain, *P. aeruginosa* PAO1, grown either planktonically or in biofilms. The Venn diagram in Fig. 1(a) shows the number of protein spots (352) present under all of four conditions tested (planktonic/0 mM CaCl₂, planktonic/10 mM CaCl₂, biofilm/0 mM CaCl₂, and biofilm/10 mM CaCl₂, labelled P-0, P-10, B-0 and B-10, respectively). Also shown in Fig. 1(a) are the numbers of unique protein spots expressed only under one condition or under overlapping conditions. Biofilm growth showed the greatest number of unique protein spots at both low and high [Ca²⁺], demonstrating that biofilm growth results in significant physiological effects on the *P. aeruginosa* PAO1 proteome, and confirming previous reports on *P. aeruginosa* biofilm formation

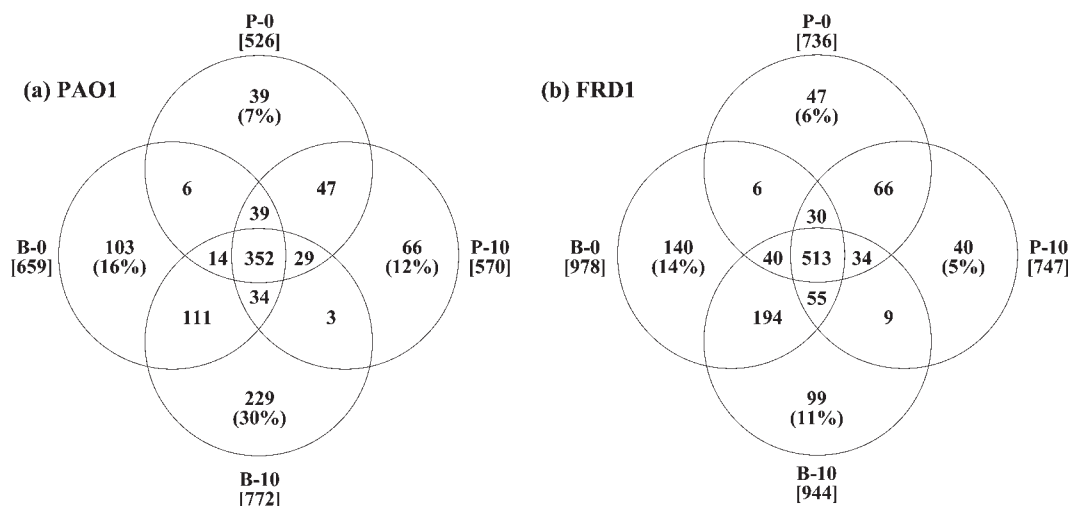


Fig. 1. Venn diagrams representing comparisons of the cytosolic proteomes of (a) *P. aeruginosa* PAO1 and (b) FRD1. Each circle represents a different growth condition. The numbers of unique protein spots, found for only one condition or for the overlapping conditions, are shown. Conditions include biofilm-associated growth with no added CaCl₂ (B-0) or with 10 mM added CaCl₂ (B-10), and planktonic growth with no added CaCl₂ (P-0) or with 10 mM CaCl₂ (P-10). The numbers in square brackets are the total numbers of protein spots detected on duplicate gels for the same conditions. The numbers in parentheses are the percentages of spots that are unique to one particular condition.

(Sauer *et al.*, 2002). Pairwise comparison showed that of the four proteomes, the two biofilm proteomes (B-0 and B-10) were most similar to each other, sharing 81% of protein spots. The two planktonic proteomes were also similar to each other, sharing 74% of the proteins. In contrast, the least similar to each other were the planktonic proteome at 0 mM CaCl₂ and the biofilm proteome at 10 mM CaCl₂, which only shared 63% of their proteins.

We observed a similar global proteome response to biofilm growth and to Ca²⁺ for the mucoid CF isolate, *P. aeruginosa* FRD1, demonstrating that even though the mucoid strain is encapsulated in alginate, in both planktonic and biofilm culture, it is nonetheless able to respond to growth associated with a surface and dramatically change its cytosolic proteome. For this strain we resolved an average of 850 protein spots in the proteomes of planktonic and biofilm cultures (Fig. 1b). Of these protein spots, 513 proteins were detected under all four conditions. The individual conditions resulted in 40–140 unique proteins. As with the PAO1 proteomes, pair-wise comparisons showed that the most similar proteome pair was the two biofilm cultures (B-0 and B-10), which shared 94% of the proteins. The two planktonic cultures (P-0 and P-10) were similar to each other, sharing 76% of the proteins. However, the biofilm cultures shared only 69–72% of the proteins with their planktonic counterparts.

To estimate how many proteins in the *P. aeruginosa* PAO1 proteomes had changed abundances of at least twofold (including unique proteins) under the effect of [Ca²⁺] or biofilm growth, we quantitatively compared protein spot intensities in proteome pairs. Fig. 2 shows that although

biofilm growth had the greatest effect on the number of proteins with at least twofold differences in abundances (51–54% of proteins), [Ca²⁺] contributed to this effect. Whereas in planktonic culture, [Ca²⁺] resulted in

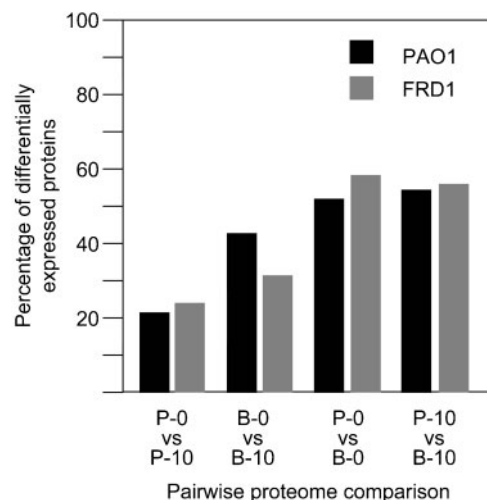


Fig. 2. Quantitative comparison of protein abundances in proteome pairs. The percentages of proteins with twofold more or less abundance compared to the total number of proteins detected are shown. The percentages correspond to averaged gels (obtained by using Progenesis software) for at least two biological replicates for each condition. Proteome comparisons are for planktonic and biofilm-associated growth with or without added CaCl₂, labelled as in Fig. 1.

differential abundances of 23 % of proteins, this increased to 43 % in biofilm cultures, demonstrating that $[Ca^{2+}]$ and biofilm growth have cumulative effects on the proteomes of *P. aeruginosa* PAO1. Similar results were observed in the pair-wise comparison of the *P. aeruginosa* FRD1 proteomes. Quantitative comparison of the spot intensities in proteome pairs showed that the number of differentially expressed proteins reached its highest level (56–60 %) in the biofilm proteomes versus their planktonic counterparts. $[Ca^{2+}]$ contributed to this effect primarily during biofilm growth.

Cluster analysis of protein abundance profiles reveals changes in response of individual proteins to environmental conditions

To characterize the responses of individual proteins to changes in environmental conditions, the normalized signal intensities of 568 differentially expressed proteins from PAO1 and 897 proteins from FRD1 were analysed by

hierarchical cluster analysis. Protein spot signal intensities generated by Progenesis software were imported into GeneSpring software. Proteins were clustered based on abundance patterns for each protein under the different growth conditions. For both strains, 12 clusters were identified, including 377 proteins from PAO1, representing 66 % of the differentially expressed proteins, and 554 proteins from FRD1, constituting 62 % of the differentially expressed proteins (Fig. 3). Clusters 1–3 combine the proteins that were more abundant during biofilm growth, either independently of $[Ca^{2+}]$ (cluster 1) or at low $[Ca^{2+}]$ (cluster 2), or high $[Ca^{2+}]$ (cluster 3). Clusters 4–6 include the proteins that have greater abundances during planktonic growth, either independently of $[Ca^{2+}]$ (cluster 4) or at low (cluster 5) or high $[Ca^{2+}]$ (cluster 6). Clusters 7 and 8 contain proteins that are influenced by $[Ca^{2+}]$, but not influenced by biofilm growth. The remaining clusters contain proteins that are reduced under one condition (cluster 9, reduced in B-0; cluster 10, reduced in B-10; cluster 11, reduced in P-0; and cluster 12, reduced in P-10).

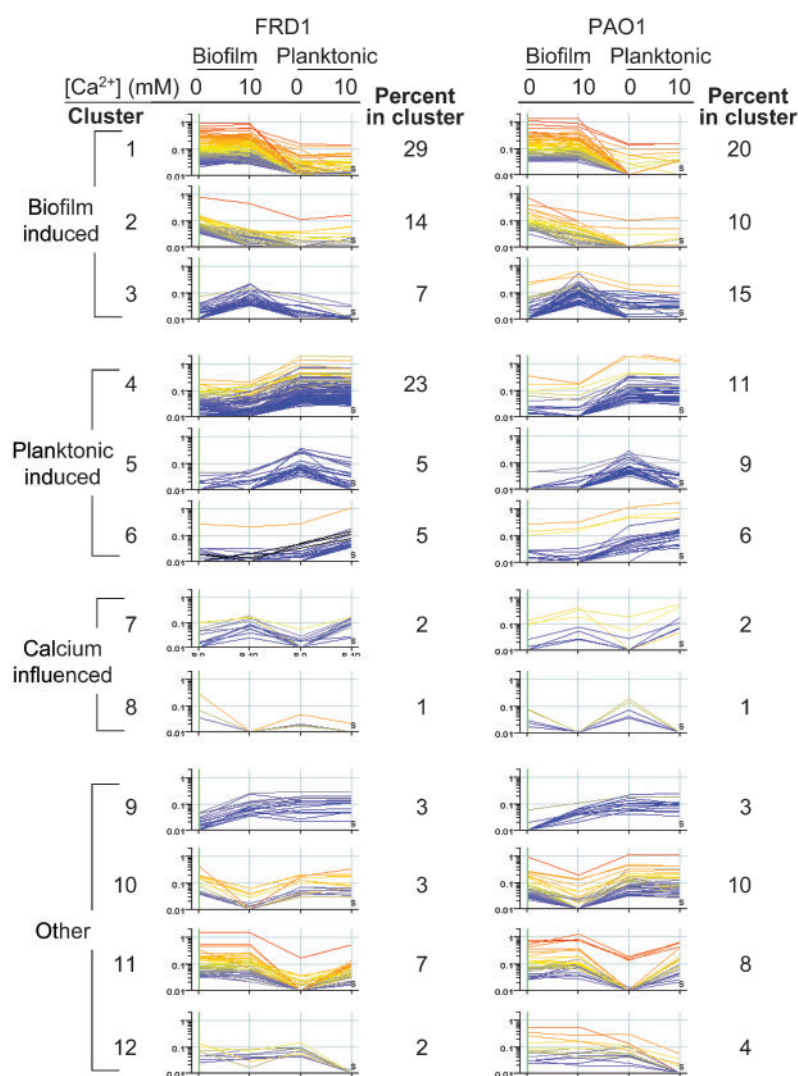


Fig. 3. Hierarchical cluster analysis of protein-spot signal intensities for the FRD1 and PAO1 proteomes. Signal intensities from averaged duplicate samples were obtained by using Progenesis software for each protein under the four conditions tested (planktonic growth at low and high $[CaCl_2]$ and biofilm growth at low and high $[CaCl_2]$). Signal intensities were exported from Progenesis Software into GeneSpring Software for cluster analysis. Proteins with similar signal intensity patterns under the four conditions were clustered together, and 12 clusters were obtained for each strain. Signal intensities for 554 proteins from FRD1 and 377 proteins from PAO1, and the percentages of proteins that grouped into each of the 12 clusters, are shown. The colours correspond to protein abundances, with red showing greatest abundance, yellow intermediate levels and blue lower abundance.

In both PAO1 and FRD1 most differentially expressed proteins (45–50%) were represented in clusters 1–3 (biofilm-induced clusters), with approximately 30% of the proteins represented in the planktonic-induced clusters (clusters 4–6). Three per cent of the proteins were positively or negatively affected by calcium independently of biofilm growth (clusters 7 and 8, respectively). The remaining proteins (25% in PAO1 and 15% in FRD1) had decreased abundance in response to one of the four conditions. Cluster analysis was used to identify protein spots most suitable for protein identification by mass spectrometry. From the PAO1 proteomes we identified 59 protein spots, including 46 unique proteins. These proteins represented eight of the 12 clusters described above. We also identified 140 proteins from the FRD1 proteomes (including 100 unique proteins) representing nine of the 12 clusters. Table 1 lists 45 proteins whose abundances were influenced by biofilm-associated growth and/or by $[Ca^{2+}]$, and the cluster for each protein.

Biofilm-induced synthesis of proteins involved in iron acquisition and storage

The level of intracellular iron or active transport of chelated iron serves as a signal for biofilm development in *P. aeruginosa* PAO1 (Banin *et al.*, 2005) and is critical for *P. aeruginosa* virulence (Musk *et al.*, 2005). For example, iron bound to the *P. aeruginosa*-derived siderophore pyochelin augments oxidant-mediated damage to pulmonary artery endothelial cells (Britigan *et al.*, 1992, 1994). Here, we identified a number of proteins involved in iron acquisition and storage that were induced by biofilm growth and/or by $[Ca^{2+}]$. Four proteins involved in the two iron-acquisition systems, PvdNOA (the high-affinity pyoverdine system) and FptA (the low-affinity pyochelin receptor protein) (Redly & Poole, 2003), shared similar abundance profiles in PAO1, highly induced by Ca^{2+} during biofilm growth (cluster 3). Southey-Pillig *et al.* (2005) also showed the presence of Pvd proteins in the proteomes of PAO1 cells at the first (PvdSQA) and second (PvdDJI) stages of biofilm maturation. Therefore, these results for PAO1 are consistent with previous reports. However, our data show that $[Ca^{2+}]$ in addition to biofilm growth contributes to the induction of these two siderophore systems (e.g. PvdN; Fig. 4). Interestingly, in FRD1, abundances of Pvd and Fpt proteins differed from those in PAO1. No detectable amounts of FptA or PvdA were seen under any of the conditions tested. However, PvdNO showed no effect due to biofilm growth, but had greater abundance due to increased $[Ca^{2+}]$ (cluster 7; Fig. 4).

Although the siderophore-mediated iron acquisition systems varied in expression between the strains, other iron uptake proteins were similar. Bacterioferritin (BfrA) and ViuB (PA2033), a protein predicted to interact with siderophores, were highly expressed in biofilms, independently of $[Ca^{2+}]$ (cluster 1; Fig. 4).

A bacterioferritin homologue, PA4880, was highly expressed in FRD1 biofilms (cluster 1) but not observed in PAO1. Two other proteins, HitA (PA4687) and PA5217, both of which are probably involved in iron transport, were induced by Ca^{2+} in both planktonic and biofilm cultures of PAO1 (cluster 7) and had reduced abundance in biofilms of FRD1 (cluster 4).

Biosynthesis and secretion of pyoverdine are regulated by means of the extracytoplasmic function (ECF) σ factor PvdS, whose expression is regulated by iron concentration and the ferric uptake regulator (Fur) (Hassett *et al.*, 1996; Ochsner *et al.*, 1995; Ochsner & Vasil, 1996; Vasil *et al.*, 1998). Our results demonstrate that $[Ca^{2+}]$ influences the production of iron-scavenging proteins and products, but the role of $[Ca^{2+}]$ in this process is not clear. Calcium may play a direct role in signalling production of these proteins, but it may also have an indirect effect by causing an increase in thickness of biofilms. This effect may be more pronounced in FRD1, where Ca^{2+} causes a more dramatic effect on biofilm thickness (Sarkisova *et al.*, 2005), and perhaps results in a higher percentage of biofilm-associated cells undergoing iron starvation. These results confirm the importance of iron and iron scavenging in *P. aeruginosa* biofilm development, as both strains produced iron-acquiring proteins and siderophores during this process. The strains varied in the particular iron-acquiring proteins produced.

Quorum sensing and quinolone signalling

Quorum sensing is an important component in the development of *P. aeruginosa* biofilms (Davies *et al.*, 1998). Many of the proteins we identified as having increased abundances in biofilms are regulated by the LasR and/or RhIR quorum-sensing regulators (Table 1). In addition, we identified PqsB protein, involved in biosynthesis of *Pseudomonas* quinolone signal (PQS), a third *P. aeruginosa* signalling compound, as increased in abundance in FRD1 biofilms (Fig. 4). The abundance of PqsB was relatively constant under the different growth conditions for PAO1, although twofold higher in planktonic culture at high $[Ca^{2+}]$. Quinolone signalling has been shown to be involved in the regulation of iron-starvation-responsive genes, possibly through its ability to chelate iron (Bredenbruch *et al.*, 2006), and therefore may influence the production of iron-scavenging proteins as observed above. It is also involved in regulation of certain stress-responsive genes; and in FRD1, protein abundances of a number of stress-responsive genes correlated with the abundance of PqsB (Table 1 and described below).

Biofilm growth affects the abundance of proteins involved in oxidative stress and protein post-translational modification

Oxidative stress has been reported previously to be interlinked with iron availability (Hassett *et al.*, 1995,

Table 1. Proteins identified by MASCOT-based analysis of MALDI-TOF-generated mass spectra

Protein name	Gene name	PA no.	Genetic context	Cluster PAO1/FRD1	MASCOT score*	No. of peptides by QS†	Regulated	Normalized signal intensity (NV)‡							
								PAO1				FRD1			
								P-0	P-10	B-0	B-10	P-0	P-10	B-0	B-10
Iron acquisition and storage															
PvdN	<i>pvdN</i>	2394	<i>pvd</i> , pyoverdine synthesis operon	3/7	481	16		N	N	0.065	0.19	0.019	0.046	0.007	0.019
PvdO	<i>pvdO</i>	2395	<i>pvd</i> operon	3/7	104	10		0.078	0.087	0.051	0.13	N	0.15	N	0.087
PvdA, L-ornithine N ⁵ -oxygenase	<i>pvdA</i>	2386	<i>pvd</i> operon	3/N	304	18	P	N	N	N	0.048	N	N	N	N
Fe(III)-pyochelin receptor precursor	<i>fptA</i>	4221	<i>fptAB</i> and <i>pchEFR</i> , pyochelin synthesis operon	3/N	278	21	P	N	N	N	0.19	N	N	N	N
Hypothetical protein (predicted siderophore-interacting protein)	Predicted <i>viuB</i>	2033	Single gene	1/1	101	10		0.03	0.033	0.073	0.20	0.031	0.09	0.16	0.15
Bacterioferritin	<i>bfrA</i>	4235	<i>katA</i> Single gene	1/1	198	9		N	N	0.08	0.31	N	N	0.21	0.13
Probable bacterioferritin		4880	Single gene	N/1	75	9	P, L, R	N	N	N	N	N	N	0.38	0.23
Ferric iron-binding periplasmic protein HitA	<i>hitA</i>	4687	<i>hitB</i>	7/4	320	12		0.053	0.16	0.11	0.19	0.19	0.19	0.085	0.12
Probable binding protein component of ABC iron transporter		5217	ABC iron transport and glycine cleavage system	7/4	198	15		0.027	0.11	0.025	0.075	0.067	0.054	N	0.019
Quinolone signal response															
Probable β -keto-acyl-acyl-carrier protein synthase	<i>pqsB</i>	0997	<i>pqsABCDE</i> operon	6/1	186	7	P, L, R	0.059	0.11	0.063	0.047	0.044	0.04	0.09	0.12
Oxidative stress															
Catalase	<i>kata</i>	4236	<i>bfrA</i>	1/11	323	20	P	N	0.01	0.044	0.07	0.014	0.031	0.063	0.07
Catalase HPII	<i>katE</i>	2147	Hypothetical	N/4	331	23	P, L, R	N	N	N	N	0.25	0.25	0.044	0.042
Alkyl hydroperoxide reductase subunit C	<i>ahpC</i>	0139	<i>ahpF</i>	7/4	264	9	P	0.13	0.61	0.43	0.82	0.43	0.45	0.29	0.29
Probable peroxidase		3529	Single gene	3/N	176	17		N	N	N	0.14	N	N	N	N
Probable antioxidant protein		3450	Single gene	2/N	311	12		N	N	0.096	0.005	N	N	N	N

Table 1. cont.

Protein name	Gene name	PA no.	Genetic context	Cluster PAO1/FRD1	MASCOT score*	No. of peptides matched	Regulated by QS†	Normalized signal intensity (NV)‡							
								PAO1				FRD1			
								P-0	P-10	B-0	B-10	P-0	P-10	B-0	B-10
PTM/chaperones/stress response															
GroEL protein	<i>groEL</i>	4385	<i>groES</i>	N/1	260	17		N	N	N	N	0.11	0.14	0.31	0.31
Heat-shock protein GrpE	<i>grpE</i>	4762	<i>dnaK</i>	N/1	75	7	P	N	N	N	N	N	0.008	0.089	0.093
Predicted universal stress protein UspA		4352	Hypothetical	1/1	634	21		0.092	0.096	0.22	0.18	N	N	0.25	0.21
Predicted universal stress protein UspA		3309	RNA helicase <i>hepA</i>	1/1	582	15		N	N	0.58	0.53	N	N	0.67	0.81
Regulatory protein TypA (predicted GTPase involved in stress response)	<i>typA</i>	5117	Thiazole biosynthesis, <i>thiI</i>	1/1	575	29		N	N	0.17	0.17	N	N	0.036	0.21
DnaK protein	<i>dnaK</i>	4761	<i>dnaJ</i> , <i>grpE</i> , <i>dapB</i>	3/1	159	20	P	N	N	N	0.11	0.024	0.027	0.077	0.066
Trigger factor	<i>tig</i>	1800	<i>clpPX</i> proteases	3/N	128	10		N	N	N	0.12	N	N	N	N
Heat-shock protein HtpG	<i>htpG</i>	1596	Hypothetical	3/N	285	24		N	N	N	0.07	N	N	N	N
Thiol : disulfide interchange protein DsbA	<i>dsbA</i>	5489	Hypothetical	11/4	557	11		0.08	0.18	0.19	0.25	0.44	0.39	0.065	0.12
Probable carbamoyl transferase		2069	Transporter	N/1	553	24	R	N	N	N	N	0.021	0.014	0.18	0.22
Transcriptional regulator (two-component system)	<i>phoP</i>	1179	<i>oprH</i> and <i>phoQ</i>	2/N	331	13		N	N	0.14	N	N	N	N	N
Protein degradation															
PvdS-regulated endoprotease, lysyl class	<i>prpL</i>	4175	Single gene	1/1	202	10	L, R	N	N	0.26	0.33	N	0.044	0.17	0.17
ATP-dependent Clp protease proteolytic subunit	<i>clpP</i>	1801	<i>tig-clpX</i>	11/1	128	10		0.092	0.13	0.19	0.23	0.071	0.088	0.19	0.19
Predicted protease	<i>thiJ</i>	1135	Hypothetical	7/4	128	10		0.012	0.025	0.026	0.095	0.046	0.059	0.029	0.01
Protease PfpI	<i>pfpI</i>	0355	Hypothetical	7/4	496	10	L, R	0.057	0.091	0.045	0.14	0.33	0.27	0.037	0.06
Probable protease		4171	Hypothetical	N/4	235	8	L, R	N	N	N	N	0.2	0.12	N	N
Phenazine biosynthesis															
Probable phenazine biosynthesis protein	<i>phzB1</i>	4211	Phenazine biosynthesis (<i>phz</i>) operon	1/1	108	8	L, R	N	N	0.17	0.088	N	N	0.24	0.19

Table 1. cont.

Protein name	Gene name	PA no.	Genetic context	Cluster PAO1/FRD1	MASCOT score*	No. of peptides matched	Regulated by QS†	Normalized signal intensity (NV)‡							
								PAO1				FRD1			
								P-0	P-10	B-0	B-10	P-0	P-10	B-0	B-10
Probable phenazine biosynthesis protein	<i>phzF1</i>	4215	<i>phz</i> operon	1/1	230	7	L, R	0.078	0.087	0.19	0.097	N	N	0.28	0.27
Probable pyridoxamine 5'-phosphate oxidase	<i>phzG1</i>	4216	<i>phz</i> operon	1/1	340	9	L, R	N	N	0.03	0.25	N	N	0.027	0.03
Flavin-containing monooxygenase	<i>phzS</i>	4217	<i>phz</i> operon	1/1	345	17	P, L, R	N	0.012	0.21	0.042	0.007	0.037	0.096	0.14
Phenazine biosynthesis protein PhzD	<i>phzD1</i>	4213	<i>phz</i> operon	1/1	215	8	L, R	N	0.023	0.097	0.20	N	N	0.14	0.28
Probable phenazine biosynthesis protein	<i>phzB2</i>	1900	<i>phz</i> operon	1/1	196	9	P	N	N	0.72	0.61	N	N	0.24	0.19
Probable pyridoxamine 5'-phosphate oxidase	<i>phzG2</i>	1905	<i>phz</i> operon	1/1	454	10	P, L, R	N	N	0.42	0.21	N	N	0.52	0.55
Polysaccharide biosynthesis/metabolism															
GDP-mannose 6-dehydrogenase AlgD	<i>algD</i>	3540	Alginate biosynthesis operon, <i>alg</i>	N/7	505	25		N	N	N	N	0.2	0.52	0.30	0.75
Serine protease MucD precursor	<i>mucD</i>	0766	Alginate regulation operon, <i>mucABC</i>	10/4	248	11		0.075	0.094	0.094	0.055	0.15	0.17	0.036	0.054
UTP-glucose-1-phosphate uridylyltransferase	<i>galU</i>	2023	Nucleotide sugar dehydrogenase	4/4	311	12		1.9	1.2	0.17	N	1.5	1.3	0.24	0.19
Probable glycosyl hydrolase	<i>glgX</i>	2160	Hypothetical	3/5	142	17	L, R	N	N	0.012	0.077	0.7	0.034	N	N
Glycogen phosphorylase	<i>glgP</i>	2144	Hypothetical	N/4	744	36	L, R	N	N	N	N	0.17	0.097	0.01	0.01
Nitrogen metabolism															
NosF protein nitrous oxide reductase	<i>nosF</i>	3394	<i>nosLYFDZR</i>	3/1	75	11		N	N	N	0.023	N	N	0.08	0.061
Urease β subunit	<i>ureB</i>	4867	<i>ureDABC</i>	2/1	75	5		N	N	0.093	0.008	N	N	0.064	0.076

N, not detected.

*MASCOT-generated probability-based Mowse score. Scores greater than 75 are significant ($P < 0.05$).†The corresponding genes were reported as being upregulated by LasI (L), RhII (R) or PQS (P) quorum sensing (QS) systems in Bredenbruch *et al.* (2006), Schuster *et al.* (2003) or Wagner *et al.* (2003).

‡Average normalized volumes over the two biological replicates under each of the tested growth conditions.

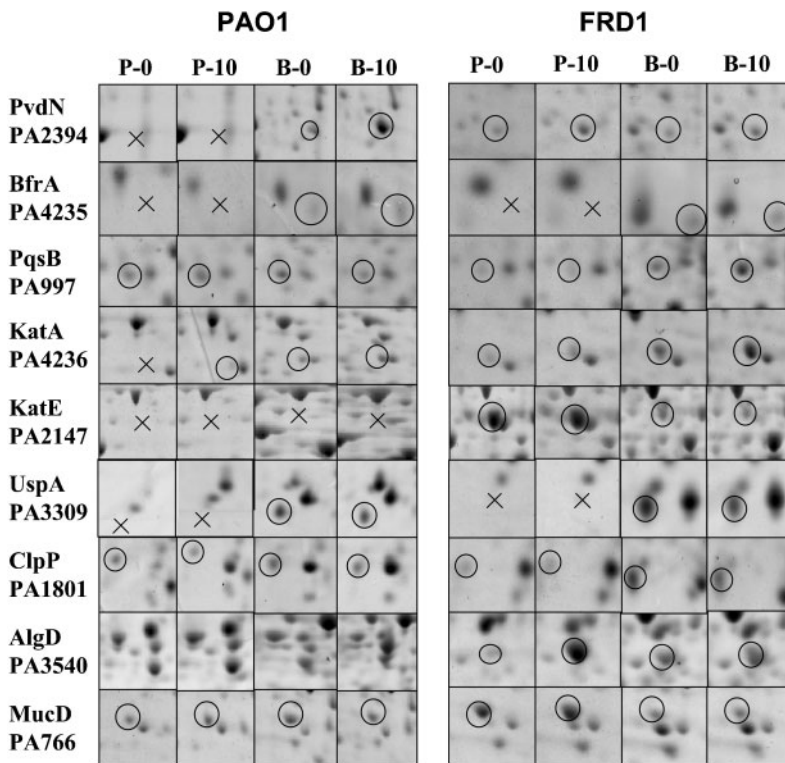


Fig. 4. Sections of 2D gels showing selected proteins in PAO1 and FRD1 proteomes. The spots from each of the four conditions tested are shown, with circles showing identified spots, and crosses showing the corresponding protein counterpart not detected under the particular condition. P-0, P-10, B-0 and B-10 are as defined in Fig. 1.

1996) and in some cases controlled by quorum-sensing regulatory circuitry (Hassett *et al.*, 1999). Biofilm cells express higher resistance to bactericidal reactive oxygen intermediates (Elkins *et al.*, 1999). We detected five antioxidant proteins with significantly differing abundances under the effects of Ca^{2+} and biofilm growth. The major catalase, KatA, was induced in biofilms in both strains (Fig. 4). This protein was also induced by Ca^{2+} in both planktonic cultures. Expression of *katA* is positively regulated by RhlR and LasR quorum sensing (Hassett *et al.*, 1999) and also influenced by quinolone signalling (Bredenbruch *et al.*, 2006). Results presented here show a direct relationship between quorum sensing, biofilm growth and amount of KatA. In FRD1, a second catalase, KatE (PA2147), showed the opposite expression profile to KatA, with sixfold higher abundance in the proteomes of planktonic cells than in the biofilms (Fig. 4). KatE was not observed in PAO1 under any of the conditions tested here.

Another oxidative-stress-responsive protein, AhpC, alkyl hydroperoxide reductase, had a very different abundance profile in the two strains. In PAO1 it was induced by Ca^{2+} in both planktonic and biofilm cells, but was little influenced by biofilm growth (cluster 7). In FRD1 it had decreased abundance in biofilm cells, and was not affected by Ca^{2+} (cluster 4). Although part of the PQS regulon (Bredenbruch *et al.*, 2006), AhpC does not correlate with the abundance profile of PqsB. In a previous comparison of mucoid and non-mucoid *P. aeruginosa* CF lung isolates, AhpC was detected only in the non-mucoid proteome (Hanna *et al.*, 2000). These discrepancies demonstrate

strain variations in oxidative stress responses of *P. aeruginosa*, and indicate complexity in the regulation of this response.

Other proteins possibly involved in oxidative stress are PA3529 and PA3450, which showed greater abundances in PAO1 biofilms, but at high and low Ca^{2+} , respectively. These proteins were not observed in the FRD1 biofilms, demonstrating that both strains responded to oxidative stress, but by the expression of different stress-responsive proteins.

Biofilm growth affects the abundance of chaperones and proteins involved in post-translational modification

Six proteins (DnaK, GroEL, GrpE, TypA and two homologues of UspA) associated with cellular stress responses, including chaperones and proteins involved in post-translational folding and stabilization, showed increased abundance in biofilm-grown cells of FRD1 (cluster 1; Fig. 4). In PAO1 six stress-response proteins (TypA, both UspA homologues, DnaK, HtpG and Tig) were also induced during biofilm growth. Three of these proteins (DnaK, HtpG and Tig) were induced in biofilms but only with elevated Ca^{2+} (cluster 3). The similarity in profiles of the chaperone/post-translational modification proteins is striking, with six out of eight proteins detected in FRD1 induced in biofilm cells, and six of eight also induced in biofilms of PAO1, but with greater dependence on $[Ca^{2+}]$.

Cellular stress-responsive proteins have been shown to be important in biofilm development. HtpG was previously shown to be induced in mature *P. aeruginosa* PAO1 biofilms (Southey-Pillig *et al.*, 2005), and DnaK has been detected in the proteome of a mucoid *P. aeruginosa* strain (Hanna *et al.*, 2000). In mycobacteria, GroEL1 is required for mycolate biosynthesis and for biofilm maturation (Ojha *et al.*, 2005). The results presented here expand on those studies by showing that many of the chaperones and post-translational modification proteins are induced during biofilm growth of both the mucoid and non-mucoid strains of *P. aeruginosa*.

Disulfide isomerase protein DsbA was induced by both Ca^{2+} and biofilm in PAO1, whereas in FRD1 it was less abundant, and induced only by calcium in biofilm cells. Previously this protein has been shown to be more abundant in the mucoid *mucA22* derivative versus wild-type PAO1 (Malhotra *et al.*, 2000), which agrees with our data for planktonic cells. The expression of *dsbA* is under σ -22 control, which is required for the activation of alginate biosynthesis genes. A deletion of *dsbA* in PAO1 resulted in reduced twitching motility and reduced accumulation of extracellular proteases, including elastase (Malhotra *et al.*, 2000), previously demonstrated to be present in the matrix material of FRD1 biofilms (Sarkisova *et al.*, 2005).

Proteases

In our previous study we showed that calcium addition resulted in increased abundance of three extracellular proteases (AprA, LasB and PrpL) in FRD1 biofilms and that these proteases are present in the alginate extracellular matrix material (Sarkisova *et al.*, 2005). Here we identified five proteases, both intracellular proteases and precursors of secreted proteases, that were influenced by Ca^{2+} and/or biofilm growth. Expression of the proteases differed between the two *P. aeruginosa* strains. PrpL is an extracellular protease, that we identified in the previous study. Here, we identified its cytoplasmic precursor as being induced in biofilms in both strains. PrpL was also induced by Ca^{2+} in planktonic FRD1 cells. Previously PrpL has been shown to be Ca^{2+} -regulated in *P. aeruginosa* PA103 (Marquart *et al.*, 2005). PrpL is regulated by PvdS (Wilderman *et al.*, 2001), which also regulates pyoverdine production.

The ClpP protease was also induced during biofilm growth in both strains (Fig. 4). However, in PAO1, ClpP also had high abundance in planktonic culture when Ca^{2+} was added, thus placing it in cluster 1 for FRD1 and cluster 11 for PAO1. Two other proteases, ThiJ and PfpI, and a putative protease, PA4171, had differing abundance profiles in the two strains. In FRD1 all three proteases were highly induced in planktonic culture and not observed in biofilms, independently of $[\text{Ca}^{2+}]$ (cluster 4). However in PAO1, ThiJ and PfpI were affected by elevated $[\text{Ca}^{2+}]$, but not by biofilm growth (cluster 7). PA4171 was

not detected in PAO1. Taken together, these data show that *P. aeruginosa* proteases are influenced by both biofilm growth and $[\text{Ca}^{2+}]$. However, strain-specific differences in the abundances of the different proteases occur, demonstrating the significance of strain variations in regulation of their production.

Biofilm-induced synthesis of pyocyanin

In our previous study, we identified biofilm-induced expression of two pyocyanin biosynthetic proteins (Sarkisova *et al.*, 2005). Here we identified seven pyocyanin biosynthetic proteins (PhzB2 and G2, and PhzB1, F1, S, D1 and G1) as highly expressed in biofilms, with little or no expression in planktonic cultures (cluster 1). The expression patterns for these proteins were similar in both *P. aeruginosa* strains. Pyocyanin mediates tissue damage and necrosis during lung infection (Lau *et al.*, 2004). Pyocyanin production is typically observed in stationary-phase cells, and is controlled by *rhl* quorum sensing (Brint & Ohman, 1995). Pyocyanin synthesis may also be enhanced by PQS, although indirectly as a result of iron depletion (Bredenbruch *et al.*, 2006; McKnight *et al.*, 2000).

Calcium but not biofilm growth induces expression of AlgD in FRD1

We have demonstrated previously that calcium causes increased expression of *algD* and increased alginate production in FRD1 (Sarkisova *et al.*, 2005). The proteomic data presented here further substantiate those results with the identification of AlgD in FRD1, which was induced by calcium but not by biofilm growth (cluster 7) (Fig. 4). Interestingly, the serine protease, MucD, which is a modulator in alginate regulation, showed significant induction in planktonic cultures (cluster 4) of FRD1 with little expression in biofilms. Little change in expression of MucD in PAO1 under the different conditions was observed. AlgD was not detected in PAO1, confirming other reports demonstrating that alginate is not the extracellular matrix material for PAO1 (Wozniak *et al.*, 2003), but that it is the primary biofilm matrix material for FRD1 (Nivens *et al.*, 2001; Sarkisova *et al.*, 2005).

Other proteins potentially involved in polysaccharide biosynthesis identified here were GalU, GlgX and GlgP. GalU was highly induced in planktonic cells in both *P. aeruginosa* strains. GlgX, a probable glycosyl hydrolase (PA2160), whose gene resides in a cluster of seven genes possibly involved in polysaccharide degradation, was only detected in PAO1 biofilm cells, where it was induced by Ca^{2+} . These results are consistent with the PAO1 transcriptional studies of Waite *et al.* (2006). However, in FRD1 GlgX showed the opposite expression profile and was only detected in planktonic cells, where it was less abundant in the presence of Ca^{2+} . GlgP, a glycogen phosphorylase that catalyses glycogen cleavage by removing glucose units from polysaccharide outer chains (Alonso-Casajus *et al.*, 2006),

also showed increased abundance in planktonic cultures of FRD1. Deletion of *glgP* in *Escherichia coli* has been shown previously to be correlated with the presence of longer external chains in the polysaccharide accumulated by cells (Alonso-Casajus *et al.*, 2006). GlgP is encoded on a gene cluster adjacent to *katE*, which shows an identical abundance profile in FRD1 (increased expression in planktonic cells).

Nitrogen metabolism

NosF, N₂O reductase (PA3394), involved in nitrous oxide respiration, was induced in biofilms of both strains, and influenced by Ca²⁺ in PAO1 (cluster 3). A similar profile was detected for urease beta subunit UreB (PA4867). *nosF* belongs to the six-gene *nos* operon, required for anaerobic respiration of nitrous oxide (Viebrock & Zumft, 1988). The recent finding that O₂ gradients exist across the mucus of the CF lung indicates that *P. aeruginosa* may switch to an anaerobic type of energy metabolism (Yoon *et al.*, 2002). The concentration of nitrite plus nitrate in exhaled breath condensate of CF patients has been shown to be significantly higher than in healthy controls (Ojoo *et al.*, 2005), and CF lung tissues contain increased amounts of calcium-dependent NO synthase (Belvisi *et al.*, 1995), suggesting a potential role for bacterial denitrification *in vivo*.

Concluding remarks

In summary, these data show that both a mucoid and non-mucoid strain of *P. aeruginosa* respond to biofilm-associated growth and elevated [Ca²⁺], through dramatic changes in cell physiology, as illustrated by their proteome responses. The two factors caused a cumulative effect on the proteomes of both strains. Calcium probably acts as a signalling molecule for *P. aeruginosa*, particularly during growth in biofilms. Many of the responses exhibited by the two strains were similar, with both showing changes in proteins required for iron uptake, stress response and biosynthesis of extracellular products and polysaccharides. However, the specific responses at the level of individual proteins often differed between the two strains. Thus, the two model *P. aeruginosa* strains, PAO1 and FRD1, commonly used to study infectious processes show both common and different protein changes in response to biofilm growth and elevated [Ca²⁺], and these changes represent different strategies the bacteria may use to adapt to new environments and possibly to evade host defences.

ACKNOWLEDGEMENTS

We thank Anthony Haag for providing the MALDI-TOF mass spectrometry analysis, and Kate McInnerney for assistance with GeneSpring analyses. This work was supported by Public Health Service grant AI-46588 (to M.J.F.) from the National Institute of Allergy and Infectious Diseases.

REFERENCES

- Alonso-Casajus, N., Dauvillee, D., Viale, A. M., Munoz, F. J., Baroja-Fernandez, E., Moran-Zorzano, M. T., Eydallin, G., Ball, S. & Pozueta-Romero, J. (2006). Glycogen phosphorylase, the product of the *glgP* gene, catalyzes glycogen breakdown by removing glucose units from the nonreducing ends in *Escherichia coli*. *J Bacteriol* **188**, 5266–5272.
- Banin, E., Vasil, M. L. & Greenberg, E. P. (2005). Iron and *Pseudomonas aeruginosa* biofilm formation. *Proc Natl Acad Sci U S A* **102**, 11076–11081.
- Belvisi, M., Barnes, P. J., Larkin, S., Yacoub, M., Tadjkarimi, S., Williams, T. J. & Mitchell, J. A. (1995). Nitric oxide synthase activity is elevated in inflammatory lung disease in humans. *Eur J Pharmacol* **283**, 255–258.
- Boles, B. R., Thoendel, M. & Singh, P. K. (2004). Self-generated diversity produces “insurance effects” in biofilm communities. *Proc Natl Acad Sci U S A* **101**, 16630–16635.
- Bredenbruch, F., Geffers, R., Nimtz, M., Buer, J. & Haussler, S. (2006). The *Pseudomonas aeruginosa* quinolone signal (PQS) has an iron-chelating activity. *Environ Microbiol* **8**, 1318–1329.
- Brint, J. M. & Ohman, D. E. (1995). Synthesis of multiple exoproducts in *Pseudomonas aeruginosa* is under the control of RhlR–RhlI, another set of regulators in strain PAO1 with homology to the autoinducer-responsive LuxR–LuxI family. *J Bacteriol* **177**, 7155–7163.
- Britigan, B. E., Roeder, T. L., Rasmussen, G. T., Shasby, D. M., McCormick, M. L. & Cox, C. D. (1992). Interaction of the *Pseudomonas aeruginosa* secretory products pyocyanin and pyochelin generates hydroxyl radical and causes synergistic damage to endothelial cells. Implications for *Pseudomonas*-associated tissue injury. *J Clin Invest* **90**, 2187–2196.
- Britigan, B. E., Rasmussen, G. T. & Cox, C. D. (1994). *Pseudomonas* siderophore pyochelin enhances neutrophil-mediated endothelial cell injury. *Am J Physiol* **266**, L192–L198.
- Costerton, J. W., Lewandowski, Z., Caldwell, D. E., Korber, D. R. & Lappin-Scott, H. M. (1995). Microbial biofilms. *Annu Rev Microbiol* **49**, 711–745.
- Costerton, J. W., Stewart, P. S. & Greenberg, E. P. (1999). Bacterial biofilms: a common cause of persistent infections. *Science* **284**, 1318–1322.
- Davies, D. G., Parsek, M. R., Pearson, J. P., Iglewski, B. H., Costerton, J. W. & Greenberg, E. P. (1998). The involvement of cell-to-cell signals in the development of a bacterial biofilm. *Science* **280**, 295–298.
- Denning, G. M., Railsback, M. A., Rasmussen, G. T., Cox, C. D. & Britigan, B. E. (1998). *Pseudomonas* pyocyanine alters calcium signaling in human airway epithelial cells. *Am J Physiol* **274**, L893–L900.
- Egan, M. E., Glockner-Pagel, J., Ambrose, C., Cahill, P. A., Pappoe, L., Balamuth, N., Cho, E., Canny, S., Wagner, C. A. & other authors (2002). Calcium-pump inhibitors induce functional surface expression of ΔF508-CFTR protein in cystic fibrosis epithelial cells. *Nat Med* **8**, 485–492.
- Elkins, J. G., Hassett, D. J., Stewart, P. S., Schweizer, H. P. & McDermott, T. R. (1999). Protective role of catalase in *Pseudomonas aeruginosa* biofilm resistance to hydrogen peroxide. *Appl Environ Microbiol* **65**, 4594–4600.
- Firoved, A. M. & Deretic, V. (2003). Microarray analysis of global gene expression in mucoid *Pseudomonas aeruginosa*. *J Bacteriol* **185**, 1071–1081.
- Friedman, L. & Kolter, R. (2004). Two genetic loci produce distinct carbohydrate-rich structural components of the *Pseudomonas aeruginosa* biofilm matrix. *J Bacteriol* **186**, 4457–4465.

- Halmerbauer, G., Arri, S., Schierl, M., Strauch, E. & Koller, D. Y. (2000).** The relationship of eosinophil granule proteins to ions in the sputum of patients with cystic fibrosis. *Clin Exp Allergy* **30**, 1771–1776.
- Hanna, S. L., Sherman, N. E., Kinter, M. T. & Goldberg, J. B. (2000).** Comparison of proteins expressed by *Pseudomonas aeruginosa* strains representing initial and chronic isolates from a cystic fibrosis patient: an analysis by 2-D gel electrophoresis and capillary column liquid chromatography-tandem mass spectrometry. *Microbiology* **146**, 2495–2508.
- Hassett, D. J., Schweizer, H. P. & Ohman, D. E. (1995).** *Pseudomonas aeruginosa* *sodA* and *sodB* mutants defective in manganese- and iron-cofactored superoxide dismutase activity demonstrate the importance of the iron-cofactored form in aerobic metabolism. *J Bacteriol* **177**, 6330–6337.
- Hassett, D. J., Sokol, P. A., Howell, M. L., Ma, J. F., Schweizer, H. T., Ochsner, U. & Vasil, M. L. (1996).** Ferric uptake regulator (Fur) mutants of *Pseudomonas aeruginosa* demonstrate defective siderophore-mediated iron uptake, altered aerobic growth, and decreased superoxide dismutase and catalase activities. *J Bacteriol* **178**, 3996–4003.
- Hassett, D. J., Ma, J. F., Elkins, J. G., McDermott, T. R., Ochsner, U. A., West, S. E., Huang, C. T., Fredericks, J., Burnett, S. & other authors (1999).** Quorum sensing in *Pseudomonas aeruginosa* controls expression of catalase and superoxide dismutase genes and mediates biofilm susceptibility to hydrogen peroxide. *Mol Microbiol* **34**, 1082–1093.
- Hentzer, M., Teitzel, G. M., Balzer, G. J., Heydorn, A., Molin, S., Givskov, M. & Parsek, M. R. (2001).** Alginate overproduction affects *Pseudomonas aeruginosa* biofilm structure and function. *J Bacteriol* **183**, 5395–5401.
- Jackson, K. D., Starkey, M., Kremer, S., Parsek, M. R. & Wozniak, D. J. (2004).** Identification of *psl*, a locus encoding a potential exopolysaccharide that is essential for *Pseudomonas aeruginosa* PAO1 biofilm formation. *J Bacteriol* **186**, 4466–4475.
- Jensen, P. O., Bjarnsholt, T., Phipps, R., Rasmussen, T. B., Calum, H., Christoffersen, L., Moser, C., Williams, P., Pressler, T. & other authors (2007).** Rapid necrotic killing of polymorphonuclear leukocytes is caused by quorum-sensing-controlled production of rhamnolipid by *Pseudomonas aeruginosa*. *Microbiology* **153**, 1329–1338.
- Jesaitis, A. J., Franklin, M. J., Berglund, D., Sasaki, M., Lord, C. I., Bleazard, J. B., Duffy, J. E., Beyenal, H. & Lewandowski, Z. (2003).** Compromised host defense on *Pseudomonas aeruginosa* biofilms: characterization of neutrophil and biofilm interactions. *J Immunol* **171**, 4329–4339.
- Keren, I., Shah, D., Spoering, A., Kaldalu, N. & Lewis, K. (2004).** Specialized persister cells and the mechanism of multidrug tolerance in *Escherichia coli*. *J Bacteriol* **186**, 8172–8180.
- Lau, G. W., Ran, H., Kong, F., Hassett, D. J. & Mavrodi, D. (2004).** *Pseudomonas aeruginosa* pyocyanin is critical for lung infection in mice. *Infect Immun* **72**, 4275–4278.
- Lewis, K. (2007).** Persister cells, dormancy and infectious disease. *Nat Rev Microbiol* **5**, 48–56.
- Liu, L., Ridefelt, P., Hakansson, L. & Venge, P. (1999).** Regulation of human eosinophil migration across lung epithelial monolayers by distinct calcium signaling mechanisms in the two cell types. *J Immunol* **163**, 5649–5655.
- Lorin, M. I., Gaerlan, P. F., Mandel, I. D. & Denning, C. R. (1976).** Composition of nasal secretion in patients with cystic fibrosis. *J Lab Clin Med* **88**, 114–117.
- Lyczak, J. B., Cannon, C. L. & Pier, G. B. (2000).** Establishment of *Pseudomonas aeruginosa* infection: lessons from a versatile opportunist. *Microbes Infect* **2**, 1051–1060.
- Lyczak, J. B., Cannon, C. L. & Pier, G. B. (2002).** Lung infections associated with cystic fibrosis. *Clin Microbiol Rev* **15**, 194–222.
- Mah, T. F., Pitts, B., Pellock, B., Walker, G. C., Stewart, P. S. & O'Toole, G. A. (2003).** A genetic basis for *Pseudomonas aeruginosa* biofilm antibiotic resistance. *Nature* **426**, 306–310.
- Mai, G. T., Seow, W. K., Pier, G. B., McCormack, J. G. & Thong, Y. H. (1993).** Suppression of lymphocyte and neutrophil functions by *Pseudomonas aeruginosa* mucoid exopolysaccharide (alginate): reversal by physicochemical, alginase, and specific monoclonal antibody treatments. *Infect Immun* **61**, 559–564.
- Malhotra, S., Silo-Suh, L. A., Mathee, K. & Ohman, D. E. (2000).** Proteome analysis of the effect of mucoid conversion on global protein expression in *Pseudomonas aeruginosa* strain PAO1 shows induction of the disulfide bond isomerase, *dsbA*. *J Bacteriol* **182**, 6999–7006.
- Marquart, M. E., Dajcs, J. J., Caballero, A. R., Thibodeaux, B. A. & O'Callaghan, R. J. (2005).** Calcium and magnesium enhance the production of *Pseudomonas aeruginosa* protease IV, a corneal virulence factor. *Med Microbiol Immunol* **194**, 39–45.
- McKnight, S. L., Iglewski, B. H. & Pesci, E. C. (2000).** The *Pseudomonas* quinolone signal regulates *rhl* quorum sensing in *Pseudomonas aeruginosa*. *J Bacteriol* **182**, 2702–2708.
- Musk, D. J., Banko, D. A. & Hergenrother, P. J. (2005).** Iron salts perturb biofilm formation and disrupt existing biofilms of *Pseudomonas aeruginosa*. *Chem Biol* **12**, 789–796.
- Nivens, D. E., Ohman, D. E., Williams, J. & Franklin, M. J. (2001).** Role of alginate and its O acetylation in formation of *Pseudomonas aeruginosa* microcolonies and biofilms. *J Bacteriol* **183**, 1047–1057.
- Ochsner, U. A. & Vasil, M. L. (1996).** Gene repression by the ferric uptake regulator in *Pseudomonas aeruginosa*: cycle selection of iron-regulated genes. *Proc Natl Acad Sci U S A* **93**, 4409–4414.
- Ochsner, U. A., Vasil, A. I. & Vasil, M. L. (1995).** Role of the ferric uptake regulator of *Pseudomonas aeruginosa* in the regulation of siderophores and exotoxin A expression: purification and activity on iron-regulated promoters. *J Bacteriol* **177**, 7194–7201.
- Ohman, D. E. & Chakrabarty, A. M. (1981).** Genetic mapping of chromosomal determinants for the production of the exopolysaccharide alginate in a *Pseudomonas aeruginosa* cystic fibrosis isolate. *Infect Immun* **33**, 142–148.
- Ojha, A., Anand, M., Bhatt, A., Kremer, L., Jacobs, W. R., Jr & Hatfull, G. F. (2005).** GroEL1: a dedicated chaperone involved in mycolic acid biosynthesis during biofilm formation in mycobacteria. *Cell* **123**, 861–873.
- Ojoo, J. C., Mulrennan, S. A., Kastelik, J. A., Morice, A. H. & Redington, A. E. (2005).** Exhaled breath condensate pH and exhaled nitric oxide in allergic asthma and in cystic fibrosis. *Thorax* **60**, 22–26.
- Olson, J. C. & Ohman, D. E. (1992).** Efficient production and processing of elastase and LasA by *Pseudomonas aeruginosa* require zinc and calcium ions. *J Bacteriol* **174**, 4140–4147.
- Pier, G. B., Coleman, F., Grout, M., Franklin, M. & Ohman, D. E. (2001).** Role of alginate O acetylation in resistance of mucoid *Pseudomonas aeruginosa* to opsonic phagocytosis. *Infect Immun* **69**, 1895–1901.
- Rani, S. A., Pitts, B. & Stewart, P. S. (2005).** Rapid diffusion of fluorescent tracers into *Staphylococcus epidermidis* biofilms visualized by time lapse microscopy. *Antimicrob Agents Chemother* **49**, 728–732.
- Redly, G. A. & Poole, K. (2003).** Pyoverdine-mediated regulation of FpvA synthesis in *Pseudomonas aeruginosa*: involvement of a probable extracytoplasmic-function sigma factor, FpvI. *J Bacteriol* **185**, 1261–1265.
- Roberts, M. E. & Stewart, P. S. (2004).** Modeling antibiotic tolerance in biofilms by accounting for nutrient limitation. *Antimicrob Agents Chemother* **48**, 48–52.

- Sarkisova, S., Patrauchan, M. A., Berglund, D., Nivens, D. E. & Franklin, M. J. (2005). Calcium-induced virulence factors associated with the extracellular matrix of mucoid *Pseudomonas aeruginosa* biofilms. *J Bacteriol* **187**, 4327–4337.
- Sauer, K., Camper, A. K., Ehrlich, G. D., Costerton, J. W. & Davies, D. G. (2002). *Pseudomonas aeruginosa* displays multiple phenotypes during development as a biofilm. *J Bacteriol* **184**, 1140–1154.
- Schuster, M., Lostrich, C. P., Ogi, T. & Greenberg, E. P. (2003). Identification, timing, and signal specificity of *Pseudomonas aeruginosa* quorum-controlled genes: a transcriptome analysis. *J Bacteriol* **185**, 2066–2079.
- Southey-Pillig, C. J., Davies, D. G. & Sauer, K. (2005). Characterization of temporal protein production in *Pseudomonas aeruginosa* biofilms. *J Bacteriol* **187**, 8114–8126.
- Stewart, P. S. & Costerton, J. W. (2001). Antibiotic resistance of bacteria in biofilms. *Lancet* **358**, 135–138.
- Stover, C. K., Pham, X. Q., Erwin, A. L., Mizoguchi, S. D., Warrener, P., Hickey, M. J., Brinkman, F. S., Hufnagle, W. O., Kowalik, D. J. & other authors (2000). Complete genome sequence of *Pseudomonas aeruginosa* PA01, an opportunistic pathogen. *Nature* **406**, 959–964.
- Vasil, M. L., Ochsner, U. A., Johnson, Z., Colmer, J. A. & Hamood, A. N. (1998). The fur-regulated gene encoding the alternative sigma factor PvdS is required for iron-dependent expression of the LysR-type regulator ptxR in *Pseudomonas aeruginosa*. *J Bacteriol* **180**, 6784–6788.
- Viebrock, A. & Zumft, W. G. (1988). Molecular cloning, heterologous expression, and primary structure of the structural gene for the copper enzyme nitrous oxide reductase from denitrifying *Pseudomonas stutzeri*. *J Bacteriol* **170**, 4658–4668.
- von Ruecker, A. A., Bertele, R. & Harms, H. K. (1984). Calcium metabolism and cystic fibrosis: mitochondrial abnormalities suggest a modification of the mitochondrial membrane. *Pediatr Res* **18**, 594–599.
- Wagner, V. E., Bushnell, D., Passador, L., Brooks, A. I. & Iglewski, B. H. (2003). Microarray analysis of *Pseudomonas aeruginosa* quorum-sensing regulons: effects of growth phase and environment. *J Bacteriol* **185**, 2080–2095.
- Weite, R. D., Papakonstantinou, A., Littler, E. & Curtis, M. A. (2005). Transcriptome analysis of *Pseudomonas aeruginosa* growth: comparison of gene expression in planktonic cultures and developing and mature biofilms. *J Bacteriol* **187**, 6571–6576.
- Weite, R. D., Paccanaro, A., Papakonstantinou, A., Hurst, J. M., Saqi, M., Littler, E. & Curtis, M. A. (2006). Clustering of *Pseudomonas aeruginosa* transcriptomes from planktonic cultures, developing and mature biofilms reveals distinct expression profiles. *BMC Genomics* **7**, 162.
- Walters, M. C., III, Roe, F., Bugnicourt, A., Franklin, M. J. & Stewart, P. S. (2003). Contributions of antibiotic penetration, oxygen limitation, and low metabolic activity to tolerance of *Pseudomonas aeruginosa* biofilms to ciprofloxacin and tobramycin. *Antimicrob Agents Chemother* **47**, 317–323.
- Whiteley, M., Banger, M. G., Bumgarner, R. E., Parsek, M. R., Teitzel, G. M., Lory, S. & Greenberg, E. P. (2001). Gene expression in *Pseudomonas aeruginosa* biofilms. *Nature* **413**, 860–864.
- Wilderman, P. J., Vasil, A. I., Johnson, Z., Wilson, M. J., Cunliffe, H. E., Lamont, I. L. & Vasil, M. L. (2001). Characterization of an endo-protease (PrpL) encoded by a PvdS-regulated gene in *Pseudomonas aeruginosa*. *Infect Immun* **69**, 5385–5394.
- Wozniak, D. J., Wyckoff, T. J., Starkey, M., Keyser, R., Azadi, P., O'Toole, G. A. & Parsek, M. R. (2003). Alginate is not a significant component of the extracellular polysaccharide matrix of PA14 and PAO1 *Pseudomonas aeruginosa* biofilms. *Proc Natl Acad Sci U S A* **100**, 7907–7912.
- Yahr, T. L., Mende-Mueller, L. M., Friese, M. B. & Frank, D. W. (1997). Identification of type III secreted products of the *Pseudomonas aeruginosa* exoenzyme S regulon. *J Bacteriol* **179**, 7165–7168.
- Yoon, S. S., Hennigan, R. F., Hilliard, G. M., Ochsner, U. A., Parvatiyar, K., Kamani, M. C., Allen, H. L., DeKievit, T. R., Gardner, P. R. & other authors (2002). *Pseudomonas aeruginosa* anaerobic respiration in biofilms: relationships to cystic fibrosis pathogenesis. *Dev Cell* **3**, 593–603.

Edited by: C. Picioreanu